A micro-mechanical modelling study of drying restraint effects on the hygro-mechanics of paper sheets

A MICRO-MECHANICAL MODELLING STUDY OF DRYING RESTRAINT EFFECTS ON THE HYGRO-MECHANICS OF PAPER SHEETS

Emanuela Bosco, Ron Peerlings, Marc Geers

Eindhoven University of Technology, Eindhoven, Netherlands

SUMMARY

In this contribution we show how fibre activation and micro-buckling of fibre walls may explain, quantitatively, differences in the hygro-mechanical response of paper sheets due to the presence or absence of mechanical restraint during their fabrication. To this end, both effects are incorporated in an idealised micro-mechanical model of the fibre network. The model is used to predict the response of the network to wetting–drying cycles, as a function of the degree of restraint during production. Restrained-dried networks are predicted to exhibit an irreversible hygroscopic strain upon first wetting and a different reversible hygro-expansivity coefficient, compared with freely-dried networks, which match well with experimental values reported in the literature.

1 INTRODUCTION

It is well documented in the literature that the hygro-expansion exhibited by paper sheets in response to changing humidity conditions depends significantly on the amount of stress applied on the sheet during production, see e.g. [1, 2, 3]. The effect is most evident in experiments on hand-sheets which were dried freely or under restraint [4, 5, 6, 7]. Figure 1 illustrates schematically the observations made in such experiments. Hand-sheets which are mechanically restrained while being dried, and which hence experience tensile stress, show a non-linear dependence of the hygroscopic strain on the moisture content when they are exposed to a high relative humidity. The subsequent drying response is generally found to be quite linear. As a result, a significant irreversible shrinkage occurs during the first hygroscopic cycle after production. This irreversible shrinkage is thought to be due to the release of strains which 'dried-in' during the production under restraint. In subsequent cycles, the linear drying response of the first cycle is followed, and the response thus is reversible. Freely dried hand-sheets, on the other hand, show a fully reversible, linear hygroscopic response even in the first cycle. However, their expansivity, i.e. the slope of the hygroscopic strain versus moisture content diagram, is significantly larger compared to that of restrained-dried sheets. This effect persists even after the (irreversible) dried-in strain has been released for the restraint-dried sheets.

The precise micro-mechanical mechanisms responsible for these two phenomena, i.e. the occurrence of irreversibility and the change in hygro-expansivity due to drying restraint, are unclear. A range of microscopic mechanisms have been suggested in the literature to explain one or both of them. Among these mechanisms are (i) visco-elastic, creep-like behaviour of individual fibres at high moisture content, referred to as fibre

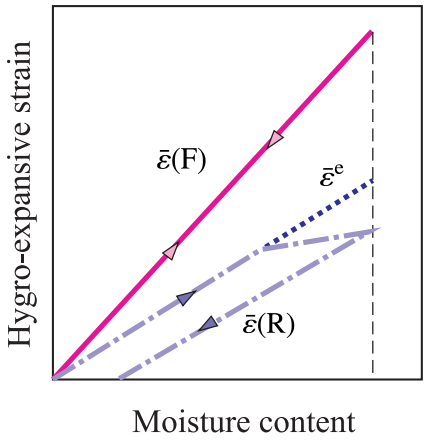

Figure 1: Schematic illustration of hygroscopic strain versus moisture content evolution as observed in wetting–drying experiments on hand-sheets which were dried freely ((F), solid line) and under restraint ((R), dash-dotted line); the dotted line marked $\bar{\varepsilon}^{e}$ represents the response of the hygro-elastic reference model of Section 2.

activation [8, 9], (ii) fibre *twisting* [10], (iii) the formation of micro-buckles, or *micro-compressions*, in the fibres due to compressive stress [11, 12], (iv) *bond degradation* effects, causing a relaxation of the mutual constraint between fibres in the network [8] and (v) differences in the *bond geometry* which have an effect on the effectiveness of the bond in relaying hygroscopic strain between the fibres [13]. However, conclusive experimental evidence as to which of these candidate mechanisms is/are the culprit(s) appears to be lacking – which may be well understood given the complexity of the material, the small spatial scales at which these phenomena occur and the small strain levels involved.

In this contribution we follow a micro-mechanical modelling strategy to explore if and how some of the more likely micro-structural mechanisms suggested in the literature could explain the macroscopically observed phenomena. We hypothesise that two of the above mechanisms are dominant: fibre activation and micro-buckling. They are incorporated at the fibre scale in a fibre network model which allows one to predict the macroscopic response of the network. Our objective is to establish whether, assuming reasonable input values for the properties of the fibres and network, the macroscopic hygroscopic strains predicted by the micro-structural model are in the range observed in experiments. If so, this confirms the two mechanisms as serious candidates and, at the same time, allows us to gain more insight in the precise way in which they affect the network's hygro-expansive properties.

Our modelling departs from a micro-structural model for the reversible hygro-mechanics of paper developed in earlier work by the authors [14]. This model has been demonstrated to predict the reversible hygro-expansion of paper sheets quite realistically, including the influence of fibre orientation distribution. Here we aim to incorporate irreversibility and the effect of drying restraint by extending the model as follows.

1. Activation of the fibres is modelled by assuming an elasto-plastic constitutive tensile response for the fibres. A kinematic hardening law is adopted, combined with a yield stress which decreases as the moisture content increases. This allows the fibres to store internal stress (and strain) as the network is dried, and to release this stress upon re-wetting.

2. The effect of micro-buckling is incorporated in the constitutive response of the fibre as a compressive buckling strength, beyond which the (incremental) lonitudinal stiffness drops to a significantly lower value. The buckling strength decreases with the moisture content, resulting in a soft compressive response of wet fibres.

Both mechanisms are modelled as time-independent. This is certainly a simplification of reality, which however is justified if the time-scale of the experiment modelled is sufficiently large, so that the system is always in equilibrium.

The model has been used to study the effect of restraint during the manufacturing of hand-sheets, as well as of machine-produced sheets – in the latter case including the effect of the anisotropy of the network. A detailed discussion of the model and results for both cases may be found in Reference [15]. Here we limit ourselves to the case of isotropic hand-sheets produced with and without restraint and discuss, mostly in qualitative terms, the evolution of the network under these two conditions, before comparing quantitatively the predicted overall hygroscopic response with experimental data taken from the literature.

This paper is organised as follows. In Section 2 we briefly review the hygro-elastic model of Reference [14] and discuss in some detail the predicted evolution of stresses in the fibres and bonds during the production of hand-sheets and during subsequent moisture cycles. This model and its response serve as a reference in our subsequent discussion on the effect of activation, in Section 3, and of micro-buckling, in Section 4. A quantitative comparison with experimental data taken from the literature follows in Section 5, before we close with concluding remarks in Section 6.

2 REFERENCE MODEL

2.1 Geometry and modelling assumptions

The micro-mechanical model which we consider is based on a highly idealised, two-dimensional network configuration. It consists of infinitely long fibres which are perfectly aligned with MD and CD and which have a constant spacing. This results in a periodic, square pattern of which one unit cell has been sketched on the left in Figure 2. The anisotropy of the network is incorporated by attributing different thicknesses to the fibres in MD and CD, which are established by integrating the fibre orientation distribution on the intervals $(-\pi/4, \pi/4)$ and $(-\pi/2, -\pi/4) \cup (\pi/4, \pi/2)$, respectively – see Figure 2 (right).

The overlap regions between the fibres in MD and CD are considered to be perfectly bonded and hence always experience the same (total) strain. This mutual constraint between the fibres, together with their highly anisotropic hygro-expansive strain, gives rise to a two-dimensional stress state in each of the fibre segments which together form the bond. The model thus acknowledges the important role of the inter-fibre bonds in the hygro-expansion of the network: it is the competition between lateral hygroscopic swelling of the fibres versus longitudinal mechanical straining which governs its overall expansion – see also below.

The free-standing parts of the fibres, in between two bonds, are assumed to be in a uniaxial stress state. At their interface with the bonds, force equilibrium is required between the axial stress in the free-standing fibre segments and the corresponding net stress in the bond.

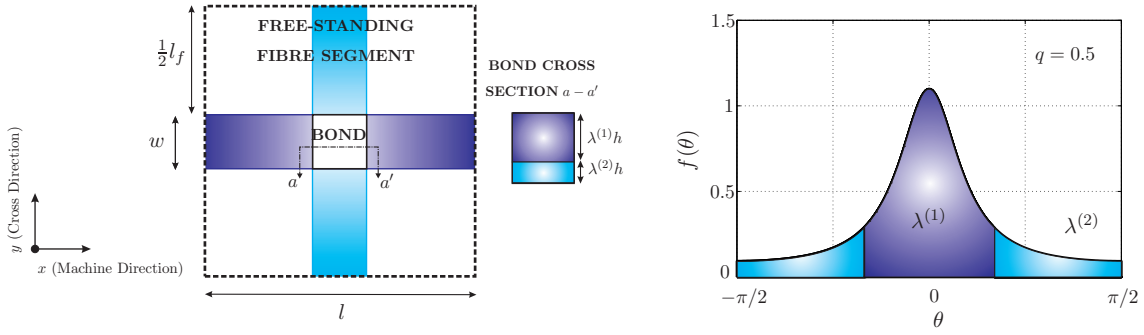

Figure 2: Sketch of the micro-structural model employed in our study: (left) geometry of a unit cell of the idealised periodic network considered and (right) fibre orientation distribution and its translation into relative thicknesses of the MD and CD fibres.

2.2 Constitutive modelling

The main purpose of the model is to allow us to define constitutive relations at the fibre scale, and nevertheless predict the sheet-scale response to hygroscopic and mechanical loading. In the hygro-elastic reference model, the strain in the fibres is considered to be the sum of two contributions: a hygroscopic part, due to variations in moisture content, and an elastic part, due to mechanical stress. The constitutive relations underlying both parts are assumed to be transversely isotropic, with their axis coinciding with the fibre axis.

For simplicity we consider here only the relevant components of the strain tensor and collect them in the vector $\boldsymbol{\varepsilon} = [\varepsilon_\mathrm{L} \;\; \varepsilon_\mathrm{T}]^\mathrm{T}$ where ε_L and ε_T denote the longitudinal and transverse strain in the fibre, respectively, i.e. the strain along the direction of the fibre axis and perpendicular to it. Given the above assumptions, the total strain may be written as

$$\boldsymbol{\varepsilon} = \boldsymbol{\varepsilon}^\mathrm{h} + \boldsymbol{\varepsilon}^\mathrm{e} \tag{1}$$

where the hygroscopic strain $\boldsymbol{\varepsilon}^\mathrm{h}$ and elastic strain $\boldsymbol{\varepsilon}^\mathrm{e}$ also consist of a longitudinal and transverse component.

The hygroscopic response is assumed to be given by the linear relationship

$$\boldsymbol{\varepsilon}^\mathrm{h} = \boldsymbol{\beta}\,\Delta\chi \tag{2}$$

where $\Delta\chi = \chi - \chi_0$ represents the moisture content, relative to the reference state in which $\chi = \chi_0$, and $\boldsymbol{\beta} = [\beta_\mathrm{L} \;\; \beta_\mathrm{T}]^\mathrm{T}$ characterises the hygro-expansivity; the latter is highly anisotropic, with a ratio of transverse/longitudinal expansivity (i.e. that perpendicular to/along the fibre axis) typically on the order of $\beta_\mathrm{T}/\beta_\mathrm{L} = 20$ [3]. Note that the model does not distinguish between water vapor and liquid water – χ is simply the mass fraction of water molecules in the sheet and $\boldsymbol{\beta}$ governs the strain induced by them irrespective of the phase they are in.

The elastic strain is given in terms of the local (fibre) stress $\boldsymbol{\sigma}$ by the generalised Hooke's law

$$\boldsymbol{\varepsilon}^\mathrm{e} = \boldsymbol{S}\,\boldsymbol{\sigma} \tag{3}$$

with the elastic compliance $\boldsymbol{S}$ given in terms of the usual engineering constants as

$$\boldsymbol{S} = \begin{bmatrix} \dfrac{1}{E_\mathrm{L}} & -\dfrac{\nu_\mathrm{TL}}{E_\mathrm{T}} \\ -\dfrac{\nu_\mathrm{LT}}{E_\mathrm{L}} & \dfrac{1}{E_\mathrm{T}} \end{bmatrix} \tag{4}$$

Its degree of anisotropy is significant too, but substantially smaller than that of the hygro-expansivity: here we use a ratio of $E_\mathrm{T}/E_\mathrm{L} = 1/6$ between the modulus in transverse direction (i.e. width and thickness) and longitudinal direction of the fibre [16]. It has been shown in Reference [14] that the Poisson effect in the fibres has little influence on the overall in-plane hygroscopic properties as predicted by the network model. For simplicity, we therefore neglect it in this study by setting $\nu_\mathrm{TL} = \nu_\mathrm{LT} = 0$. All elastic moduli are assumed to be constant, i.e. independent of the moisture content. This simplification affects the quantitative stress levels predicted in the bonds, but not the outcome of their competition, which governs the overall expansivity. For details on values of the elastic constants used, and their motivation, we refer to Reference [15].

Given the fact that the free-standing fibre segments are assumed to experience a uniaxial stress state, the above definitions may be reduced to their one-dimensional counterparts in them. As to the bonds, a two-dimensional, planar stress state exists in each of the two overlapping fibre segments (or 'layers') comprised in a bond. Note that the assumption of perfect bonding between the fibres requires the total strain (or in fact its in-plane components) to be identical between the two layers, but not the hygroscopic and elastic contributions to it, nor the stress.

2.3 Homogenisation

The moisture content in the fibres, χ, is assumed to be constant within the unit cell at all times. Its evolution in time is furthermore assumed to be known, i.e. we do not consider the moisture transport problem. An overall, sheet-scale, stress $\bar{\boldsymbol{\sigma}} = [\bar{\sigma}_\mathrm{MD}\ \bar{\sigma}_\mathrm{CD}]^\mathrm{T}$ may also be applied as a function of time. This stress may be translated into free-standing fibre stresses σ_L for the two families of fibres (in MD and CD) by multiplying its components by the respective ratios of unit cell cross section area and fibre cross section area.

Employing the constitutive equations given above, as well as internal equilibrium between the free-standing fibre segments and the bonds as discussed in Section 2.1, the strains in the free-standing fibre segments and bonds may be computed. Based on these strains, we may subsequently extract the overall strain $\bar{\boldsymbol{\varepsilon}}$ of the unit cell – and hence of the network model at the sheet scale. The details of these scale transitions are derived heuristically for the case of interest in References [15, 17] and more rigourously, based on energy equivalence between the fibre scale and the network scale, in [14].

The overall strain $\bar{\boldsymbol{\varepsilon}}$ may be decomposed into hygroscopic and elastic parts, as was done at the fibre scale in (1). Note, however, that the $\bar{\boldsymbol{\varepsilon}}^\mathrm{h}$ and $\bar{\boldsymbol{\varepsilon}}^\mathrm{e}$ thus obtained are not averages of the fibre-scale hygroscopic and elastic strains. Elastic strains generally exist at the fibre scale even at vanishing applied stress – and hence at vanishing elastic strain $\bar{\boldsymbol{\varepsilon}}^\mathrm{e}$.

2.4 Applied moisture and loading history

In this contribution we limit ourselves to modelling the production and subsequent hygroscopic testing of isotropic hand-sheets. Accordingly, we consider only networks with an

isotropic underlying fibre orientation distribution. In this case the fibres (or 'fibre bundles') in MD and CD have equal thickness/weight. Note that the network is nevertheless anisotropic due to the square pattern assumed; we however consider only the response in MD and CD. We furthermore consider only an isotropic macroscopically applied stress $\bar{\sigma}_{\mathrm{MD}} = \bar{\sigma}_{\mathrm{CD}} = \bar{\sigma}$. Under these simplifications, the MD and CD fibres are subject to exactly the same conditions and they hence show the same response. This allows one to limit the analysis to only one bond and one free-standing fibre part, cf. [15, 17].

The analysis of the network always starts in the wet state, during the production of the sheet. The fibres are assumed to be stress-free until, at a certain moisture content, the bonds are formed. We select this state, in which the bonds have just been formed, but the fibres are still stress-free, as our reference state, i.e. it has time $t = 0$, moisture content $\chi = \chi_0$ and strains $\boldsymbol{\varepsilon} = \mathbf{0}$. Figure 3 (top) illustrates the applied moisture content and stress as of this point in time, for the free as well as the restrained drying conditions. Note that, since the model has no time-dependent ingredients, the actual time which the process takes is irrelevant and the time axis of the diagram may be thought of as a pseudo-time.

In a first phase of the analysis, the moisture content is gradually reduced from its initial value χ_0 to a much lower value. This phase models the drying of the sheet during the production of the paper. In the free drying case, no external stress $\bar{\sigma}$ is applied to the network throughout this phase. Drying under restraint, on the other hand, is modelled by applying an external tensile stress $\bar{\sigma} > 0$ immediately upon the formation of the bonds, and keeping this stress constant during most of the drying. The applied stress is released towards the end of the production phase, at a low moisture content. For both restraint conditions, the production phase is thus terminated with a dry (low $\chi = \chi_{\mathrm{s}}$) network with no applied stress, indicated by 'storage' in Figure 3 (top).

The second phase of the analysis starts from this as-produced ('storage') state of the sheet and applies two consecutive moisture cycles. Two identical cycles are applied in order to reveal the possibly different responses to the first wetting cycle and subsequent cycles. In each of the two cycles, the moisture content χ is increased to a level which is significantly higher than that of the storage condition, χ_{s}, but lower than that at which the network was formed, χ_0. In the second part of each cycle the moisture content is reduced again to the storage level χ_{s}. No restraint, or external stress, is applied to either of the networks considered, i.e. the freely-dried or restrained-dried. These terms thus refer *solely* to the drying conditions during the *production* phase.

2.5 Free drying response

Consider first the case of a freely-dried network. The solid lines in Figure 3 (middle) illustrate, qualitatively, the evolution of stress in the fibres during production and during the two moisture cycles.

In the absence of any externally applied stress, the free-standing parts of the fibres are free to expand as they wish. Hence, no stress arises in them at any point in time, during production or cycling, as indicated by the solid cyan line marked $\sigma^{\mathrm{f}}(\mathrm{F})$.

Stresses do however arise in the bonded parts of the fibres, as a result of the incompatibility of their hygroscopic expansion (or contraction) in longitudinal and transverse direction. During the production stage, both fibres involved in the bond tend to contract much more in transverse direction than in longitudinal direction. The assumed full kinematic coupling within the bond area however implies that they must have *the same* strain. The difference in hygro-contraction must thus be compensated by elastic

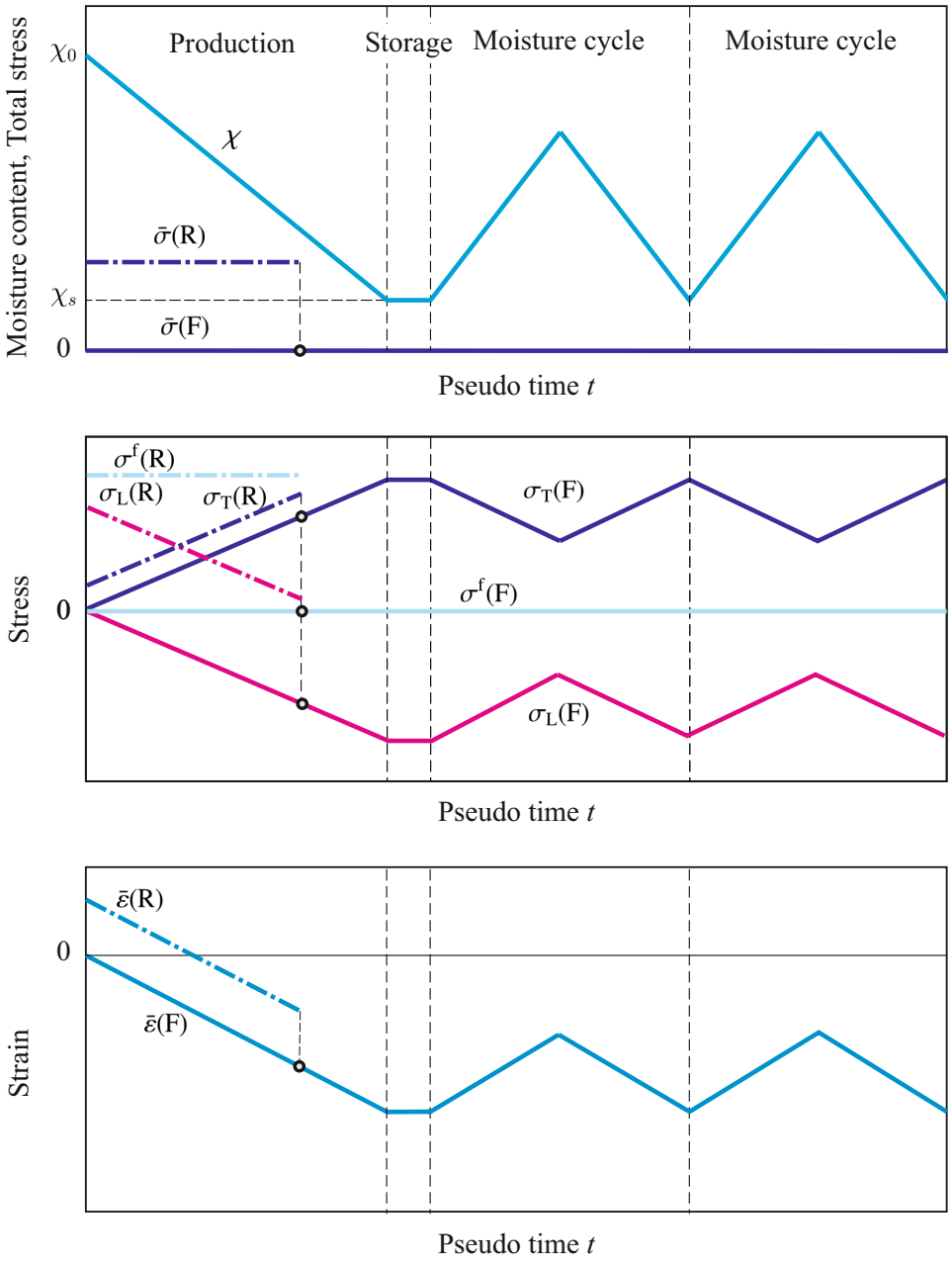

Figure 3: (top) Applied moisture content and overall stress history to mimic the production of the sheet and subsequent moisture cycling experiments, for the free drying condition ((F), solid line) and the restrained drying condition ((R), dash-dotted line). (middle) Resulting evolution of the stresses in the fibres as predicted by the hygro-elastic reference model for the free ((F), solid line) and restrained ((R), dash-dotted line) drying conditions: stress in the free-standing fibre segment, σ^f, and in the fibre parts which compose the bond, in longitudinal direction, σ_L, and transverse direction, σ_T. (bottom) Resulting overall (sheet-scale) strain of the network, $\bar{\varepsilon}$, again for the free and constrained condition.

strain, which is positive in transverse direction and negative in longitudinal direction. These elastic strains are accompanied by positive (tensile) stress in transverse and negative (compressive) stress in longitudinal direction. Given the fact that the two fibres are equally thick, these two stress levels are the exact opposite of each other – see the solid blue and magenta lines in Figure 3 (middle).

At the end of the production stage, the above mechanism has resulted in the storage of a significant amount of internal stress in the bond areas – even if the network is not subjected to any external stress. Due to these internal stresses, is significant amount of energy is also stored in the bonds. The free-standing parts of the fibres are stress-free and hence have no elastic energy.

During the wetting stages of both moisture cycles, the stresses in the bonds are reduced, because the expansion of the fibres, relative to their 'storage' state, partly removes their cause. Upon drying to the storage moisture level, the same level of internal stress is reached again as in storage, since the system is fully reversible.

The competition between longitudinal and transverse hygroscopic contraction in the bond results in a net amount of shrinkage which is a compromise between the two. Given the large contrast between the unrestricted longitudinal and transverse contractions, the resulting net bond shrinkage is significantly larger than the free longitudinal contraction of the free-standing fibre segments. The predicted overall contraction and expansion evolution of the network is therefore dominated by that of the bond.

The evolution of the resulting overall strain $\bar{\varepsilon}$ is shown in the diagram at the bottom of Figure 3. Given the linearity of the system, it scales at all times linearly with the applied moisture content change $\Delta\chi$. In terms of the strain versus moisture content diagram by which moisture cycling experiments are usually represented, the response of the hygro-elastic network is thus a straight line – see the dotted line in Figure 1. Note that the origin in this diagram represents the storage state, i.e. the moisture content starts at $\chi = \chi_s$ and the strain has been redefined relative to the storage state – as one would do in an experiment.

2.6 Restrained drying response

In the restrained drying condition, a certain amount of overall tensile stress $\bar{\sigma}$ is added during production as soon as the network (bond) has been formed – see the dash-dotted line marked (R) in Figure 3 (top). This immediately results in a tensile longitudinal stress in the free-standing fibre parts, as well as in both directions in the bonded fibre parts. In the latter, the level of stress is lower than that in the free-standing fibre parts because the force exerted by the latter is shared between the two fibres in the bond. From an energetic perspective, a significant amount of elastic energy is introduced in the system even before the start of drying.

As the moisture content is reduced, the tensile stress increases in the transverse direction and decreases in the longitudinal direction, by the same mechanism as described above for the free drying case. The applied stress (restraint) thus has the effect of shifting the two bond stresses in the direction of the tension regime – see Figure 3 (middle). In terms of the overall strain, also a positive shift is observed, which corresponds to elastically stretching the network by the applied stress $\bar{\sigma}$ – see Figure 3 (bottom).

Upon release of the restraint, i.e. removal of the applied stress, exactly the same stress state and overall strain are reached as in the free drying condition. The energy which remains in the system at this point is also identical to that of the freely dried network. The restraint thus has no effect on the remaining part of the production phase, nor on

the subsequent hygroscopic cycles. The strain versus moisture content response predicted during these cycles is the same linear response of the free drying reference case, i.e. the dotted line in Figure 1.

3 EFFECT OF FIBRE ACTIVATION

3.1 Constitutive modelling

Fibre activation, or fibre segment activation, refers to the observation that fibres dried under stress may exhibit significantly better mechanical properties compared to freely dried fibres. This phenomenon is attributed to a re-orientation of the stressed fibre's micro-fibrils, especially in the S2 layer [8, 9]. This irreversible response is a way for the fibre to relax some of the elastic energy which would otherwise be stored in it. It may be accompanied by a 'permanent' elongation on the order of 1–2%, which may however be partially removed again in an unrestrained wetting–drying cycle [8]. Our model aims at incorporating the latter effect, i.e. inelastic deformation of a fibre under the influence of restraint during drying, in the network model of the previous section.

For this purpose we extend the constitutive model of Section 2.2 with a plastic component – in longitudinal direction only. Equation (1) is thus replaced by

$$\boldsymbol{\varepsilon} = \boldsymbol{\varepsilon}^{\mathrm{h}} + \boldsymbol{\varepsilon}^{\mathrm{e}} + \boldsymbol{\varepsilon}^{\mathrm{p}} \tag{5}$$

where $\boldsymbol{\varepsilon}^{\mathrm{p}} = [\varepsilon_{\mathrm{L}}^{\mathrm{p}} \;\; 0]^{\mathrm{T}}$.

The evolution of the plastic longitudinal strain $\varepsilon_{\mathrm{L}}^{\mathrm{p}}$ is governed by a one-dimensional, rate-independent, linear kinematic hardening plasticity model in which the yield stress depends on the moisture content. The kinematic hardening models the storage of internal stress, and energy, in the fibre when it is plastically deformed (activated). The moisture dependent yield stress allows this internal stress to cause reverse plasticity (de-activation) at high moisture content, when the yield stress is low, even in the absence of externally applied stress.

The yield criterion involves solely the longitudinal stress component σ_{L}:

$$\left|\sigma_{\mathrm{L}} - K\varepsilon_{\mathrm{L}}^{\mathrm{p}}\right| - \sigma_0\left(1 - \frac{\chi}{\chi_0}\right) \leq 0 \tag{6}$$

where the equality enables plastic yielding and the response remains hygro-elastic otherwise. The product $K\varepsilon_{\mathrm{L}}^{\mathrm{p}}$ represents the back-stress, with the constant K the (kinematic) hardening modulus. This modulus characterises how much energy is stored plastically in the fibre wall as its plastic deformation increases. The second term in (6) represents the yield stress. It decays linearly with the moisture content χ, from a dry value σ_0 to zero at a critical moisture content χ_0.

The flow rule follows via normality as

$$\dot{\varepsilon}_{\mathrm{L}}^{\mathrm{p}} = \dot{\gamma}\,\mathrm{sgn}\big(\sigma_{\mathrm{L}} - K\varepsilon_{\mathrm{L}}^{\mathrm{p}}\big) \tag{7}$$

where the plastic multiplier $\dot{\gamma} \geq 0$ may be obtained, as usual, by enforcing the consistency condition, i.e. by requiring that the equality continues to hold in (6) during yielding.

3.2 Free drying response

In the absence of restraint during the production phase, the response of the model with activation enabled is expected to be identical to that of the hygro-elastic reference model

– compare the solid line curves in Figure 4 with those in Figure 3. The stresses which build up in the bond during drying never reach the yield stress, which increases at the same time due to the drying. The bond thus remains elastic, during the production phase as well as during the subsequent wetting cycles. And the free-standing fibre segments remain stress-free throughout because no external stress is applied. The overall strain evolution is thus exactly that of the reference model – see Figure 4 (bottom), and the dotted line in Figure 1 for the resulting strain versus moisture content response.

3.3 Restrained drying response

A different situation may arise if an external stress (restraint) is applied during the production-phase drying, as indicated by the dash-dotted line in Figure 4 (top). Like in the hygro-elastic case of Figure 3, the applied stress results in a shift towards tension of the stresses in the bond and, more importantly, a significant amount of tensile stress in the free-standing fibre parts, Figure 4 (middle). Since early in the process, when the fibres are still wet, their yield stress (i.e. their resistance against activation) is low, the free-standing fibre segments experience plastic deformation due to this tensile stress. In the model, a positive plastic strain $\varepsilon_{\mathrm{L}}^{\mathrm{p}}$ is induced in the free-standing fibre segments as soon as the external stress is applied, i.e. at the beginning of the analysis. At the same time, the corresponding amount of internal stress (back-stress) is generated. The occurrence of plastic strain is visible in the macro-scale strain as sketched in Figure 4 (bottom) as a vertical shift of $\bar{\varepsilon}$ in the restrained-dried case (i.e. the dash-dotted cyan line) with respect to that of the elastic reference (dotted grey).

As the network is further dried, the yield stress increases to the point where, once the the restraint is removed, part of this plastic strain remains. This implies that the free-standing fibre segments have a certain amount of internal stress and strain in the as-produced, 'storage' state. In terms of energy, a certain amount of plastic energy is stored in them, which may later be released if the hygro-mechanical loading dictates so. The fibre segments which are involved in the bond have experienced no plasticity and have thus contracted as in the elastic reference case. The net effect is that the network has contracted less than in the free drying case (and than in the reference model) – compare the dash-dotted and solid curves in Figure 4 (bottom).

Once the moisture content is increased in the first hygroscopic cycle, the yield stress drops again. This may at some point during the wetting stage result in yielding in the reverse direction (i.e. contraction), even though the freestanding fibre is stress-free ($\sigma_{\mathrm{L}} = 0$). It is the internal stress, or in terms of the model the back-stress $K\varepsilon_{\mathrm{L}}^{\mathrm{p}}$, which drives this reverse yielding. As the wetting continues, part of the internal stress and strain present in the free-standing fibre part are released – and hence the plastically stored energy in them. At the sheet-scale this results in $\bar{\varepsilon}$ approaching that of the free drying case. Note that in the example shown here some plastic strain also remains.

During the second part of the first cycle the network is dried, and hence the remaining plastic strain is 'dried in' again. At the end of the first cycle, a lower strain is observed than at the start of the cycle (i.e. than the storage strain). Relative to the storage state, an irreversible, net contraction has thus occurred, allowing the system to reach a state of lower energy. Note that this contraction has taken place without any external stress being applied. In terms of the strain versus moisture content diagram of Figure 1, it would result in exactly the response marked by (R), i.e. a non-linear (actually, bi-linear) wetting response followed by a linear drying response, which together result in a net shrinkage of the sheet during the first moisture cycle.

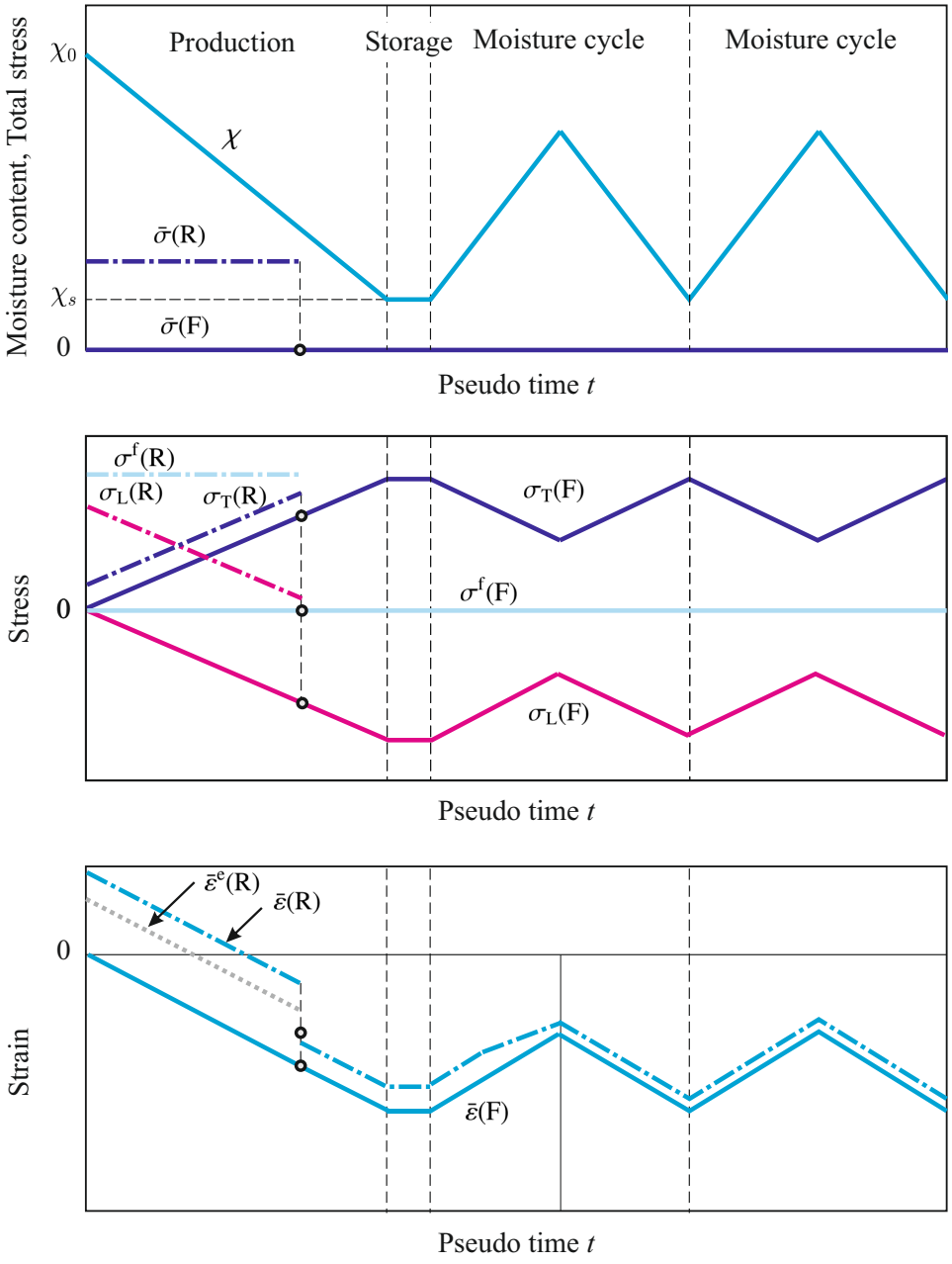

Figure 4: (top) Moisture and stress history applied to the model with activation – identical to that used for the reference model (cf. Figure 3), but repeated for clarity. Solid lines, marked with (F) refer to free drying and dash-dotted lines, marked (R), to restrained drying. (middle) Predicted evolution of the stresses in the free-standing and bonded parts of the fibres; these, too, coincide with those of the reference model, although the tensile stress in the free-standing fibre parts now results in activation/plasticity. (bottom) Resulting overall (sheet-scale) strain evolution of the network. The hygro-elastic response of Figure 3 is shown as a dotted line (and marked $\bar{\varepsilon}^e$) for comparison.

In the second moisture cycle the plasticity is never activated anymore, because the peak moisture content reached during this cycle coincides with that of the first and all plastic strain which can be released at this moisture content has already been released in the first cycle. The strain induced during this cycle is thus fully reversible and no further net contraction occurs anymore (Figure 4 (bottom)). The strain versus moisture content response is linear again, and follows, up and down, the drying part of the first cycle in Figure 1.

Note that the slopes of the initial wetting part as well as the drying part of the cycle as sketched in Figure 1 coincide with that of the reference model. Activation, as modelled here, thus results in an irreversible strain shift, but no change of the reversible expansivity.

Having established that the introduction of kinematically hardening plasticity as a way to model fibre activation results in irreversible hygroscopic strain release in the first moisture cycle, it is now interesting to observe how the magnitude of the effect depends on the parameters of the plasticity model. The main quantity of influence turns out to be the ratio of the dry yield stress and the hardening modulus, $\xi = \sigma_0/K$ [15]. Figure 5 shows the predicted moisture cycle response, taking the storage condition as reference, for three values of this ratio: a reference value of $\xi = 0.01$, as well as a lower and a higher value, $\xi = 0.005$ and $\xi = 0.015$, respectively. Clearly, a larger value of ξ allows the system to store more plastic strain and hence to exhibit a larger irreversible shrinkage in the first wetting cycle.

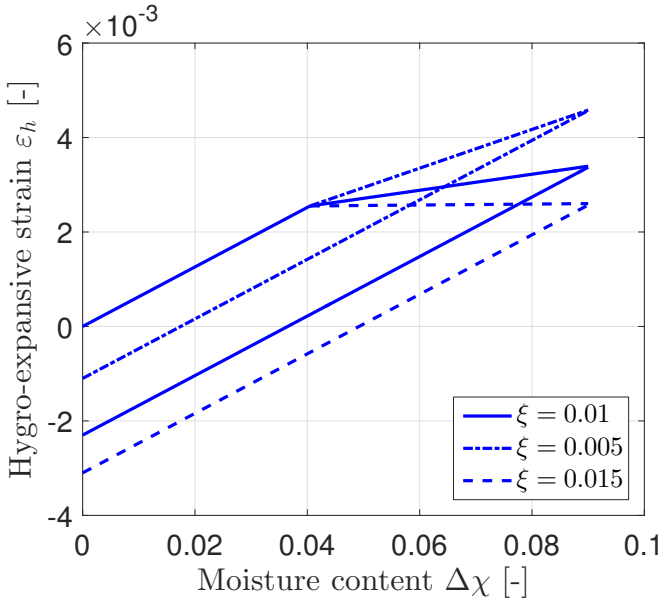

Figure 5: Effective strain $\bar{\varepsilon} - \bar{\varepsilon}_\mathrm{s}$ versus moisture content variation $\Delta\chi = \chi - \chi_\mathrm{s}$ during a moisture cycle, as predicted by the model with activation, for three different levels of the ratio $\xi = \sigma_0/K$.

4 EFFECT OF MICRO-BUCKLING

4.1 Constitutive modelling

Micro-buckles, sometimes also referred to as micro-compressions, are wrinkles or local buckles which have been observed in fibre walls within the bonding area [11, 12, 18]. They are thought to be induced by compressive stresses in longitudinal direction of the bonded fibres, which arise due to transverse drying shrinkage of the other fibre involved in the bond. These compressive stresses may trigger bending of the amorphous regions between the cellulose fibrils, that can easily be plasticized and thus act as plastic hinges. The occurrence of buckles allows the system to lower the amount of stored energy compared with the unbuckled state. Micro-buckles appear to be largely reversible: they can be released if the system is wetted again [12]. This may be understood by realizing that even though dissipative processes may be involved, e.g. the plastic hinge formation referred to above, these processes would be very localised in space and hence contribute little to the overall response of the fibre wall. Furthermore, they would be active only in the formation of the micro-buckles and not so much during their unloading and reloading in the course of hygroscopic cycles.

Rather than modelling the formation of buckles in detail, we incorporate their effect in an aggregated sense in the constitutive model of the fibres. This is consistent with our objective of modelling their effect on the overall network response and with the relative simplicity of our model. For this purpose, the constitutive model is furnished with a moisture-dependent buckling strength in compression, in terms of the longitudinal stress σ_{T}. The post-buckling response is reversible and linear, but with a significantly lower modulus than in the unbuckled state.

The constitutive model may be formalised by rephrasing the elastic response in rate form according to (cf. (3))

$$\dot{\boldsymbol{\varepsilon}}^{\mathrm{e}} = \boldsymbol{S}\,\dot{\boldsymbol{\sigma}} \tag{8}$$

with the elastic compliance $\boldsymbol{S}$ now given by (cf. (4) together with the assumption $\nu_{\mathrm{TL}} = \nu_{\mathrm{LT}} = 0$):

$$\boldsymbol{S} = \begin{bmatrix} \dfrac{1}{C_{\mathrm{L}}} & 0 \\ 0 & \dfrac{1}{E_{\mathrm{T}}} \end{bmatrix} \tag{9}$$

and

$$C_{\mathrm{L}} = \begin{cases} E_{\mathrm{L}} & \text{if } \sigma_{\mathrm{T}} > \tilde{\sigma} \\ \tilde{E}_{\mathrm{L}} & \text{otherwise} \end{cases} \tag{10}$$

In these expressions E_{L} and $\tilde{E}_{\mathrm{L}}$ denote respectively the pre and post-buckling modulus in longitudinal direction; $\tilde{\sigma}$ is the current buckling strength, i.e. the stress at which buckling occurred, or at which it would occur at the current moisture content. This quantity must be updated during the analysis according to the evolution of stress and moisture content – see Reference [15] for details. Its dependence on the moisture content is bi-linear, with a relatively steep slope at low moisture content and a weaker dependence at high moisture content – see again [15] for details.

This micro-buckling model shows some similarity with the activation model of Section 3.1. For constant moisture content and monotonic loading both models exhibit a bi-linear stress–strain response. However, two important differences are that (i) micro-buckling model is active only in compression whereas plastic straining may be positive or

negative and (ii) the buckling model is fully reversible – all strain is fully recovered upon unloading, unlike the elasto-plastic activation model.

4.2 Free drying response

For the model with micro-buckling of the fibres enabled, let us again first consider the free drying response. As in the reference model, drying the initial, wet network results in an increasing amount of compressive longitudinal stress in the bonded fibre parts (as well as tensile transverse stress). Since the buckling strength is low at high moisture content, this compressive stress may result in micro-buckling early on in the drying process. The resulting drop of the incremental stiffness in longitudinal direction causes a slower increase of compressive stress in longitudinal direction – and hence, because of equilibrium, also of the tensile stress in transverse direction. This is visible in Figure 6 (middle) as a departure of the solid curves from the dotted reference solution. The energy stored in the network (in the bonds) during drying is lower than in the reference model without buckling included.

The micro-buckles thus produced in the bonds are preserved at lower moisture content, where the buckling strength is higher, and persist in the 'storage' state. In fact, they persist also during the subsequent moisture cycles, provided the applied moisture level is not too high.

Because of the micro-buckling, the longitudinal incremental stiffness of the bonded fibre parts has dropped – possibly, depending on their post-buckling stiffness, even below their transverse stiffness. As a consequence, the fibres' expansivity in transverse direction, which is much larger than that in longitudinal direction, has a more pronounced influence in the bond's expansivity than in the initial, unbuckled bond. The bonds which have experienced micro-buckling are thus predicted to respond stronger to moisture changes, i.e. have a higher hygro-expansivity.

As a result, the sheet-scale expansivity is also increased relative to the reference model. This is visible in Figure 6 (bottom) as a steeper change of strain for a given change of moisture content than observed for the reference model, e.g. during the moisture cycles. In terms of the hygroscopic strain versus moisture content diagram of Figure 1 this implies a steeper slope, such as the one marked $\bar{\varepsilon}(\mathrm{F})$.

Note that the change in expansivity due to micro-buckling as discussed above is not accompanied by any irreversible strain, as sketched in Figure 1, and one merely observes a steeper slope – no vertical shift. This was to be expected, given the fact that the buckling response has been modelled as fully reversible. If a (fully) irreversible constitutive model had been adopted to model the effect of micro-buckling, this would have shown up as (mechanical) hysteresis during the moisture cycles.

It is instructive to vary the post-buckling stiffness $\tilde{E}_\mathrm{L}$ relative to the pre-buckling value of E_L. Figure 7 shows the hygroscopic strain response, relative to the storage condition, to a moisture cycle for three values of the ratio $\kappa = E_\mathrm{L}/\tilde{E}_\mathrm{L}$. The value of $\kappa = 10$, i.e. the post-buckling stiffness is ten times smaller than the pre-buckling modulus, is considered to be a reasonable estimate – although no experimental data is available to support this claim. The two other values considered here are the two extremes: $\kappa = 1$ implies no difference between the two values, and hence no effect of buckling, while $\kappa \to \infty$ implies $\tilde{E}_\mathrm{L} = 0$, i.e. no post-buckling stiffness at all. The macroscopic expansivity, i.e. the slope of the curves, changes by approximately a factor of three between these two extremes. We can therefore conclude that the predicted network expansivity is only mildly sensitive to the post-buckling stiffness.

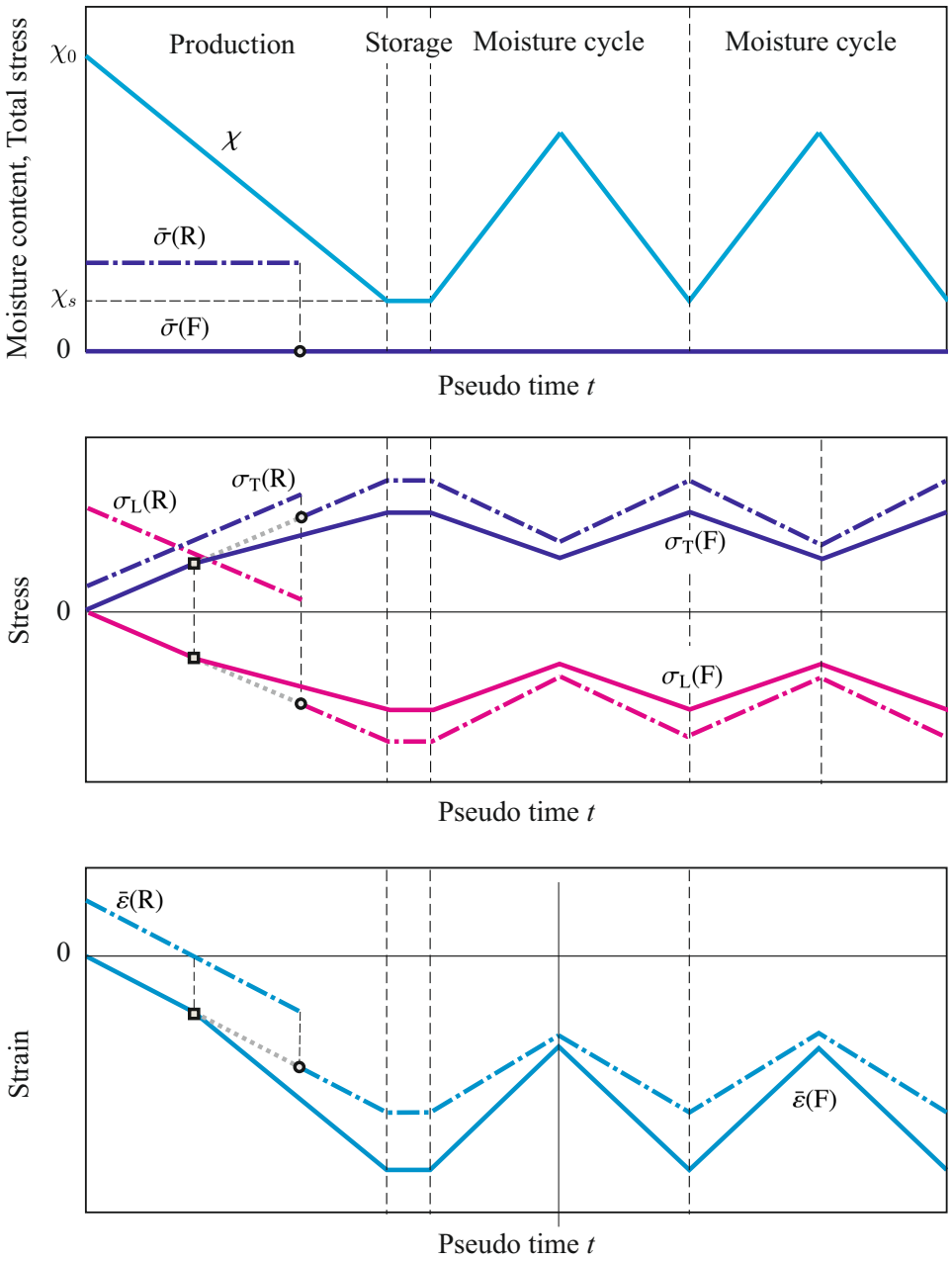

Figure 6: (top) Applied moisture and stress history – repeated for clarity. (middle) Evolution of the stresses in the free-standing and bonded parts of the fibres as predicted by the model with micro-buckling for the free drying and restrained drying conditions (solid and dash-dotted lines, respectively). The response of the reference model is also shown, by dotted lines, for comparison. (bottom) Resulting overall (sheet-scale) strain evolution of the network, together with that of the reference model.

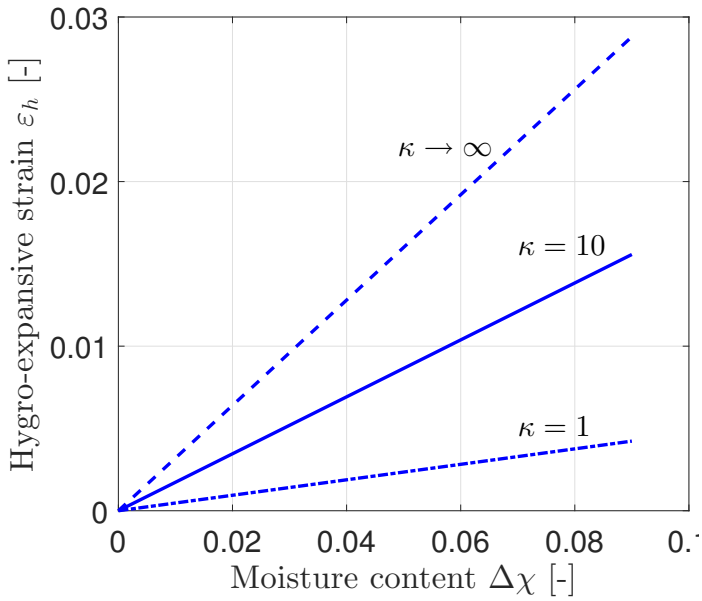

Figure 7: Predicted effective response during a moisture cycle for the model with micro-buckling, for three different levels of post-buckling stiffness, characterised by the ratio $\kappa = E_{\mathrm{L}}/\tilde{E}_{\mathrm{L}}$.

4.3 Restrained drying response

An external stress (or restraint) applied during the initial drying phase has the effect of moving the bond stresses in the direction of tension – compare the dash-dotted lines in Figure 6 (middle) with the solid lines in the same diagram. If the applied stress is sufficiently high, it may (partly) cancel the compressive longitudinal stress in the bonded fibres – see again Figure 6 (middle), in which the magenta dash-dotted line stays in the tension regime. If in addition the buckling strength has increased sufficiently, due to drying, by the time the restraint is released, no micro-buckling occurs in the bonds.

Under these conditions, the bonds in the as-produced network, in the 'storage' state, thus have the same properties as those in the elastic reference model of Section 2. As a result, no change in the overall reversible hygro-expansivity coefficient is anticipated compared with the elastic model, and this expansivity is thus smaller than that of the freely-dried network.

5 COMPARISON WITH EXPERIMENTS

Our results so far suggest that the two candidate mechanisms considered, fibre activation and micro-buckling, allow one to explain at least qualitatively the differences in hygroscopic response between freely-dried and restrained-dried hand-sheets as observed in experiments (see also Figure 1).

Activation is predicted to play a role only in the restrained condition. It results in the storage of internal strain in free-standing fibre segments, which may be released as irreversible shrinkage in a moisture cycle experiment. In the free drying condition, no internal strain is generated; hence a freely-dried network exhibits a fully reversible hygro-mechanical response.

Micro-buckling, on the other hand, occurs in the free drying condition. It results in a

significantly larger reversible hygro-expansivity than one would observe without buckling. Applying a stress, or restraint, during production may prevent the formation of micro-buckles and thus results in a lower expansivity.

A question which remains is whether the predicted magnitude of these effects is also realistic when compared with experimental observations. This question is answered by Figure 8, which compares the predicted overall network response in quantitative terms with the experimental results reported by Larsson and Wagberg [7] – for the freely-dried case on the left and restrained-dried on the right. Plotted is in both cases the overall strain, relative to the storage condition, versus moisture content during a wetting-drying cycle.

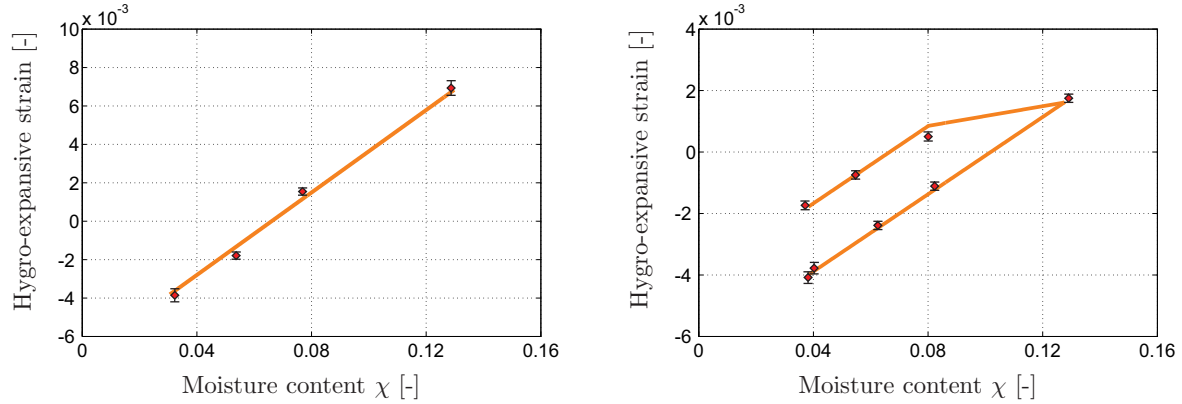

Figure 8: Comparison of the predicted hygro-expansive behaviour as a function of moisture content with experimental data presented in [7], for (left) freely-dried hand-sheets and (right) restrained-dried hand-sheets. The curves represent the predicted response, the markers denote the experimental data for untreated, virgin fibres.

The fibre-scale properties used in the model where possible have been taken from various sources in the literature – see Reference [15] for details. An educated guess was made for parameters for which no experimental data was found, e.g. the yield stress σ_0, hardening modulus K and post-buckling stiffness $\tilde{E}_{\mathrm{L}}$. In particular, values of $\xi = 0.01$ and $\kappa = 10$ have been used for the ratios discussed earlier.

The response of the freely-dried sheet is reversible, in the model and experimentally, see Figure 8 (left). In the model, micro-buckling occurs, but no activation. The predicted network hygro-expansivity, $\bar{\beta} = 0.105$ compares well with the measured hygroscopic strains.

In the restrained-dried case, the model predicts no micro-buckling and the initial hygro-expansivity hence is lower than for the freely dried netowrk: $\bar{\beta} = 0.063$. The amount of released internal strain in the experiment is comparable with the calculated irreversible strain of 2.3×10^{-3}. In the model this irreversible strain is due to activation of the freestanding fibre segments.

6 CONCLUDING REMARKS

Predictions made by the proposed microstructural model demonstrate that the hypothesised micro-mechanical mechanisms may indeed be responsible for drying restraint effects observed in paper sheets. The effect of activation of free-standing fibre segments is able

to explain, also quantitatively, irreversible hygroscopic strain levels observed in experiments. Micro-buckling in the bonds provides a viable explanation for the difference in reversible hygro-expansivity which is also observed in experiments.

We wish to emphasise that this is *no proof* that these micro-mechanical mechanisms are indeed responsible for the macroscopically observed behaviour – other possible explanations exist and in fact some of them might be modelled in very similar ways. Whether this would also lead to a similar quantitative agreement remains to be seen.

As far as the mechanisms considered here are concerned, a remaining question is how their prediction is affected by the simplicity, mostly geometrically, of the micro-structural model employed. Real fibre networks are much more random than the perfectly aligned fibres assumed here. And they are three-dimensional rather than two-dimensional. Both simplifications certainly have an effect on the micro-mechanical mechanisms modelled here and on their propagation to the macro-scale.

The influence of randomness has recently been studied in [19] for the hygro-elastic case (cf. the reference model of Section 2), by generating random two-dimensional periodic cell models and systematically computing their effective hygro-mechanical properties in a fashion which is similar to earlier work by Salminen et al. [2]. This random model is currently begin extended with the activation and micro-buckling models proposed here.

The extension to three dimensions remains an open question, which presents many additional technical and scientific challenges.

REFERENCES

[1] T. Wahlström. Influence of shrinkage and stretch during drying on paper properties. *Paper Technology*, 41(6):39–46, 2000.

[2] L. I. Salminen, M. J. Alava, S. Heyden, P-J. Gustafsson, and K.J. Niskanen. Simulation of network shrinkage. *Nordic Pulp and Paper Research Journal*, 17(2):105–110, 2002.

[3] K. J. Niskanen. *Paper physics*. Papermaking Science and Technology. Fapet Oy, Helsinki, Finland, 2nd edition, 2008.

[4] T. Uesaka, C. Moss, and Y. Nanri. The characterization of hygroexpansivity of paper. *Journal of Pulp and Paper Science*, 18(1):J11–J16, 1992.

[5] Y. Nanri and T. Uesaka. Dimensional stability of mechanical pulps – dying shrinkage and hygroexpansivity. *TAPPI Journal*, 76(6):62–66, 1993.

[6] T. Uesaka. General formula for hygroexpansion of paper. *Journal of Materials Science*, 29(9):2373–2377, 1994.

[7] P. A. Larsson and L. Wagberg. Influence of fibre-fibre joint properties on the dimensional stability of paper. *Cellulose*, 15(4):515–525, 2008.

[8] C.A. Jentzen. The effect of stress applied during drying on some of the properties of individual pulp fibers. *Tappi*, 47(7):412–418, 1964.

[9] A. K. Vainio and Paulapuro H. Interfiber bonding and fiber segment activation in paper. *BioResources*, 2(3):442–458, 2007.

[10] P. P. Gillis and Mark R. E. Analysis of shrinkage, swelling and twisting of pulp fibers. *Cellulose Chem. Technol.*, 7:209–234, 1973.

[11] D. Page and P.A. Tydeman. A new theory of the shrinkage, structure and properties of paper. In *Formation and Structure of Paper*, pages 397–421. Trans. Oxford Symp., London: F. Bolam Ed, 1962.

[12] H. W. Haslach. A model for drying-induced microcompressions in paper: Buckling in the interfiber bonds. *Composites Part B: Engineering*, 27(1):25 – 33, 1996.

[13] T. Uesaka and D. Qi. Hygroexpansivity of paper - Effects of fibre to fibre bonding. *Journal of Pulp and Paper Science*, 20(6):J175–J179, 1994.

[14] E. Bosco, R. H. J. Peerlings, and M. G. D. Geers. Predicting hygro-elastic properties of paper sheets based on an idealized model of the underlying fibrous network. *International Journal of Solids and Structures*, 56-57:43–52, 2015.

[15] E. Bosco, R. H. J. Peerlings, and M. G. D. Geers. Explaining irreversible hygroscopic strains in paper: a multi-scale modelling study on the role of fibre activation and micro-compressions. *Mechanics of Materials*, 91:76–94, 2015.

[16] A. Bergander and L. Salmén. Cell wall properties and their effects on the mechanical properties of fibers. *Journal of Materials Science*, 37(1):151–156, 2002.

[17] E. Bosco, M. V. Bastawrous, R. H. J. Peerlings, J. P. H. Hoefnagels, and M. G. D. Geers. Bridging network properties to the effective hygro-expansive behaviour of paper: experiments and modelling. *Philosophical Magazine*, 95(28-30):3385–3401, 2015.

[18] H. W. Haslach. The moisture and rate-dependent mechanical properties of paper: A review. *Mechanics of Time-Dependent Materials*, 4(3):169–210, 2000.

[19] E. Bosco, R. H. J. Peerlings, and M. G. D. Geers. Hygro-mechanical properties of paper fibrous networks through asymptotic homogenization and comparison with idealized models. *Mechanics of Materials*, 108:11–20, 2017.